10B.

GAMMA RAY SPECTROMETRIC METHODS IN URANIUM EXPLORATION — THEORY AND OPERATIONAL PROCEDURES

R.L. Grasty
Geological Survey of Canada, Ottawa

Grasty, R.L., Gamma ray spectrometric methods in uranium exploration — theory and operational procedures; in Geophysics and Geochemistry in the Search for Metallic Ores; Peter J. Hood, editor; Geological Survey of Canada, Economic Geology Report 31, p. 147-161, 1979.

Abstract

Many of the instrumental and operational problems in airborne gamma ray surveys have been solved and reliable data can now be provided. Multi-channel recording is an integral part of many survey operations and can be used to minimize energy calibration problems due to spectral drift and can also be used to increase sensitivity for uranium. In areas where suitable lakes cannot be found, upward looking crystals have proven essential for monitoring variations of atmospheric background from decay products of radon. To correct for variations of cosmic radiation due to changes in topographic relief, an energy window above that of the natural gamma ray emissions from the ground is often used.

Construction of concrete calibration pads and the utilization of calibration strips has greatly facilitated the standardization of airborne data from different detector configurations. The energy and angular distribution of the natural gamma-radiation field over uniformly radioactive ground can now be calculated reliably. By incorporating the detector response, the sensitivity of a particular system to each of the radioelements can be evaluated.

Résumé

De nombreux problèmes reliés aux instruments et aux travaux de levés aériens à rayons gamma ont été résolus; il est maintenant possible d'en obtenir des données sûres. L'enregistrement multicanal fait partie intégrante de nombreux travaux de levés et peut servir à réduire au minimum les problèmes d'étalonnage énergétique dus à la dérive spectrale; il peut aussi être utilisé pour accroître la sensibilité à l'uranium. Dans des régions où il n'est pas possible de trouver des lacs convenables, des cristaux d'orientation ascendante se sont avérés essentiels pour le contrôle des variations de la zone de fond atmosphérique à partir de la famille radioactive du radon. On utilise souvent, pour corriger les variations de radiation cosmique dues aux changements du relief topographique, une fenêtre énergétique au-dessus de celle des émissions naturelles de rayons gamma provenant du sol.

La construction de blocs d'étalonnage en béton et l'utilisation de bandes d'étallonnage ont grandement facilité la normalisation des données aériennes à partir des diverses configurations décelées par le détecteur. L'énergie et la distribution angulaire du champ naturel de rayonnement gamma au-dessus d'un terrain radioactif uniforme peuvent maintenant être calculées avec justesse. En joignant les données du détecteur, on peut évaluer la sensibilité d'un système à chacun des radioéléments.

THE NATURAL GAMMA-RADIATION FIELD

Basic Considerations

While studying the phosphorescence of various materials Becquerel discovered that an invisible radiation was emitted by several uranium salts that was capable of traversing thin layers of opaque material and fogging a photographic plate (Becquerel, 1896a, b). Soon afterwards Schmidt (1898) and Curie (1898) independently observed that a similar radiation was emitted by compounds of thorium. Through the work of Villard (1900), Rutherford (1903), and Strutt (1903) it was shown that three characteristic types of radiation were emitted, alpha, beta, and gamma radiation. Potassium was found by Campbell and Wood to emit beta radiation in 1906 although it was not until 1927 that it was observed by Kolhorster to emit gamma radiation (Campbell and Wood, 1906; Campbell, 1907; Kolhorster, 1928).

Alpha rays or alpha particles are doubly positively-charged helium nuclei and are absorbed by a few centimetres of air. Beta particles are electrons carrying unit negative charge, are more penetrating and can travel up to a metre or so. Gamma radiation, an electromagnetic radiation similar in nature to X-rays is strongly penetrating and was found from measurements by Wulf (1910) on the Eiffel Tower to be capable of ionizing air at heights of 300 m.

The absorption of gamma radiation takes place in three distinct ways, by the photoelectric effect, by scattering, and by pair production.

In the photoelectric effect the energy of the gamma ray is completely absorbed through the emission of an electron. The scattering process known as the Compton effect takes place when a gamma ray photon collides with an electron, imparts part of its energy to the electron, and is scattered at an angle to the original direction of the incident photon. This process predominates for moderate gamma ray energies in a wide range of materials. The third process, pair production can only take place if the incident photon has an energy greater than 1.02 MeV, since 1.02 MeV is necessary for the creation of an electron-positron pair. This interaction predominates at high energies particularly in materials of high atomic number. Because most materials (rocks, air and water) encountered in airborne radioactivity measurements have a low atomic number and because most natural gamma rays have moderate to low energies (less than 2.62 MeV) Compton scattering is the predominant absorption process occurring between the source of the radioactivity and the detector.

If a collimated beam of radiation of intensity I is incident upon an absorbing layer of thickness dx, the amount of radiation absorbed dI is proportional both to dx and to I so that:

$$dI = -\mu I dx$$

The proportional factor μ is a characteristic property of the medium known as the linear attenuation coefficient and is a function of the gamma ray energy. If the intensity I has the value I_o when no absorbing material is present then it follows that

$$I = I_o e^{-\mu x}$$

The thickness of absorbing material that reduces the intensity to half its original value is called the half-value thickness ($x_{1/2}$). It follows from the previous equation that

$$x_{1/2} = \frac{\log_e 2}{\mu} = \frac{0.693}{\mu}$$

Table 10B.1 shows the calculated half-thicknesses and mass attenuation coefficients at various energies, for water, air and rock (Hubbell and Berger, 1968). The mass attenuation coefficient is the linear attenuation coefficient divided by the density of the material. At aircraft altitudes of 100 m or more the intensity of gamma rays below 0.10 MeV emitted by rocks and soils in the ground will be considerably reduced and dominated by Compton-scattered high-energy gamma radiation. It is apparent that the measurement of natural radioactivity must be carried out within a few hundred metres of the ground and only gamma rays originating from a few tens of centimetres below the surface of the ground can be detected.

All rocks and soils are radioactive and emit gamma radiation. The three major sources are:

1. Potassium-40, which is 0.12 per cent of the total potassium and emits gamma ray photons of energy 1.46 MeV.
2. Decay products in the uranium-238 decay series.
3. Decay products in the thorium-232 decay series.

The gamma ray spectrum from the uranium and thorium decay series is extremely complex. Table 10B.2 and 10B.3 show the principal gamma rays over 100 KeV that are emitted by uranium-238 and thorium-232 in equilibrium with their decay products as tabulated by Smith and Wollenberg (1972). Their relative abundance, measured as photons per disintegration is also indicated. Tables 10B.4 and 10B.5 show the two radioactive series together with the principal emissions and half lives of the decay products.

Table 10B.1

Mass attenuation coefficients and half thickness for various gamma ray energies in air, water and concrete

Photon Energy MeV	Mass Attenuation Coefficient (cm2/g)			Half Thickness[a]		
	Air[b]	Water	Rock[c]	Air[d] (m)	Water (cm)	Rock[e] (cm)
0.01	4.82	4.99	26.5	1.11	0.139	0.01
0.10	0.151	0.168	0.171	35.5	4.13	1.62
0.15	0.134	0.149	0.140	40.0	4.65	1.98
0.20	0.123	0.136	0.125	43.6	5.10	2.22
0.30	0.106	0.118	0.107	50.6	5.87	2.59
0.40	0.0954	0.106	0.0957	56.2	6.54	2.90
0.50	0.0868	0.0966	0.0873	61.8	7.18	3.18
0.60	0.0804	0.0894	0.0807	66.7	7.75	3.43
0.80	0.0706	0.0785	0.0708	75.9	8.83	3.92
1.0	0.0635	0.0706	0.0637	84.4	9.82	4.35
1.46	0.0526	0.0585	0.0528	102	11.8	5.25
1.5	0.0517	0.0575	0.0519	104	12.1	5.34
1.76	0.0479	0.0532	0.0482	112	13.0	5.75
2.0	0.0444	0.0493	0.0447	121	14.1	6.20
2.62	0.0391	0.0433	0.0396	137	16.0	7.00
3.0	0.0358	0.0396	0.0365	150	17.5	7.60

a – The thickness of material which reduced the intensity of the beam to half its initial value.

b – 75.5% N, 23.2% O, 1.3% Ar by weight.

c – Composition of typical concrete, see Hubbell and Berger (1968).

d – For air at 0°C and 76 cm of Hg with a density of 0.001293 g/cm^3.

e – Density of concrete is 2.5 g/cm^3.

Table 10B.2

Principal[a] gamma rays over 100 KeV emitted by uranium in equilibrium with its decay products

Isotope[b]	γ-Energy (KeV)	Intensity[c]	Isotope[b]	γ-Energy (KeV)	Intensity[c]
Th-234	115	0.42	Bi-214	786	0.29
U-235	144	0.48	Bi-214	806	1.10
Ra-223	144	0.14	Bi-214	821	0.16
Ra-223	154	0.24	Bi-214	826	0.13
U-235	163	0.22	Pb-211	832	0.14
U-235	186	2.52	Bi-214	839	0.59
Ra-226	186	3.90	Pb-214	904	0.59
U-235	205	0.22	Bi-214	934	3.10
Th-227	236	0.51	Bi-214	964	0.37
Pb-214	242	7.60	Pa-234M	1001	0.83
Th-227	256	0.28	Bi-214	1052	0.33
Pb-214	259	0.80	Bi-214	1070	0.26
Ra-223	269	0.61	Bi-214	1104	0.16
Rn-219	271	0.45	Bi-214	1120	15.0
Pb-214	275	0.70	Bi-214	1134	0.25
Pb-214	295	18.9	Bi-214	1155	1.70
Ra-223	324	0.16	Bi-214	1208	0.47
Th-227	330	0.13	Bi-214	1238	6.10
Ra-223	338	0.12	Bi-214	1281	1.50
Bi-211	351	0.60	Bi-214	1304	0.11
Pb-214	352	36.3	Bi-214	1378	4.30
Bi-214	387	0.31	Bi-214	1385	0.80
Bi-214	389	0.37	Bi-214	1402	1.50
Rn-219	402	0.29	Bi-214	1408	2.60
Pb-211	405	0.18	Bi-214	1509	2.20
Bi-214	406	0.15	Bi-214	1539	0.53
Bi-214	427	0.10	Bi-214	1543	0.34
Bi-214	455	0.28	Bi-214	1583	0.73
Pb-214	462	0.17	Bi-214	1595	0.30
Pb-214	481	0.34	Bi-214	1600	0.34
Pb-214	487	0.33	Bi-214	1661	1.16
Rn-222	511	0.10	Bi-214	1684	0.24
Pb-214	534	0.17	Bi-214	1730	3.20
Bi-214	544	0.10	Bi-214	1765	16.7
Pb-214	580	0.36	Bi-214	1839	0.37
Bi-214	609	42.8	Bi-214	1848	2.30
Bi-214	666	14.0	Bi-214	1873	0.22
Bi-214	703	0.47	Bi-214	1890	0.10
Bi-214	720	0.38	Bi-214	1897	0.18
Bi-214	753	0.11	Bi-214	2110	0.10
Pa-234M	766	0.31	Bi-214	2119	1.30
Bi-214	768	4.80	Bi-214	2204	5.30
Pb-214	786	0.86	Bi-214	2294	0.33
			Bi-214	2448	1.65

a – Photons with an intensity greater than 0.1%.
b – Decaying isotope.
c – Decays per 100 decays of the longest lived parent.

Table 10B.3

Principal[a] gamma rays over 100 KeV emitted by thorium in equilibrium with its decay products

Isotope[b]	γ-Energy (KeV)	Intensity[c]	Isotope[b]	γ-Energy (KeV)	Intensity[c]
Pb-212	115	0.61	Bi-212	727	6.66
Ac-228	129	3.03	Ac-228	755	1.14
Th-228	132	0.26	Tl-208	763	0.61
Ac-228	146	0.23	Ac-228	772	1.68
Ac-228	154	1.02	Ac-228	782	0.56
Ac-228	185	0.11	Bi-212	785	1.11
Ac-228	192	0.13	Ac-228	795	5.01
Ac-228	200	0.36	Ac-228	830	0.64
Ac-228	204	0.18	Ac-228	836	1.88
Ac-228	209	4.71	Ac-228	840	10.2
Th-228	217	0.27	Tl-208	860	4.32
Tl-208	234	0.12	Bi-212	893	0.37
Pb-212	239	44.6	Ac-228	904	0.90
Ra-224	241	3.70	Ac-228	911	30.0
Tl-208	253	0.25	Ac-228	944	0.11
Ac-228	270	3.90	Ac-228	948	0.13
Tl-208	277	2.34	Bi-212	952	0.18
Ac-228	279	0.24	Ac-228	959	0.33
Bi-212	288	0.34	Ac-228	965	5.64
Pb-212	300	3.42	Ac-228	969	18.1
Ac-228	322	0.26	Ac-228	988	0.20
Bi-212	328	0.14	Ac-228	1033	0.23
Ac-228	328	3.48	Ac-228	1065	0.15
Ac-228	332	0.49	Bi-212	1079	0.54
Ac-228	338	12.4	Tl-208	1094	0.14
Ac-228	341	0.44	Ac-228	1096	0.14
Ac-228	409	2.31	Ac-228	1111	0.36
Ac-228	440	0.15	Ac-228	1154	0.17
Bi-212	453	0.37	Ac-228	1247	0.59
Ac-228	463	4.80	Ac-228	1288	0.12
Ac-228	478	0.25	Ac-228	1459	1.08
Ac-228	504	0.22	Ac-228	1496	1.09
Ac-228	510	0.51	Ac-228	1502	0.60
Tl-208	511	8.10	Bi-212	1513	0.31
Ac-228	523	0.13	Ac-228	1557	0.21
Ac-228	546	0.23	Ac-228	1580	0.74
Ac-228	562	1.02	Ac-228	1588	3.84
Ac-228	571	0.19	Bi-212	1621	1.51
Ac-228	572	0.17	Ac-228	1625	0.33
Tl-208	583	31.0	Ac-228	1630	2.02
Ac-228	651	0.11	Ac-228	1638	0.56
Ac-228	675	0.11	Ac-228	1666	0.22
Ac-228	702	0.20	Ac-228	1686	0.11
Ac-228	707	0.16	Bi-212	1806	0.11
Ac-228	727	0.83	Ac-228	1887	0.11
			Tl-208	2614	36.0

a – With more than 0.1 decays per 100 decays of the longest lived parent.
b – Decaying isotope.
c – Decays per 100 decays of the longest lived parent.

Table 10B.4

The U-238 series decay chain

Isotope	Radiation	Half Life
U^{238}	α	4.507×10^9 y
↓ Th^{234}	β	24.1 d
↓ Pa^{234}	β	1.18 m
↓ U^{234}	α	2.48×10^5 y
↓ Th^{230}	α	7.52×10^4 y
↓ Ra^{226}	α	1600 y
↓ Rn^{222}	α	3.825 d
↓ Po^{218}	α	3.05 m
↓ Pb^{214}	β	26.8 m
↓ Bi^{214}	β	19.7 m
↓ Po^{214}	α	1.58×10^{-4} s
↓ Pb^{210}	β	22.3 y
↓ Bi^{210}	β	5.02 d
↓ Po^{210}	α	138.4 d
↓ Pb^{206}	stable	

Isotopes constituting less than 0.2 per cent of the decay products are omitted.

Table 10B.5

The Th-232 decay series

Isotope	Radiation	Half Life
Th^{232}	α	1.39×10^{10} y
↓ Ra^{228}	β^-	6.7 y
↓ Ac^{228}	β^-	6.13 h
↓ Th^{228}	α	1.91 y
↓ Ra^{224}	α	3.64 d
↓ Rn^{220}	α	55.3 s
↓ Po^{216}	α	0.158 s
↓ Pb^{212}	β^-	10.64 h
Bi^{212} (36%)	β^- (64%), α (36%)	60.5 m
Po^{212}	α	3.04×10^{-7} s
64% Tl^{208}	β^-	3.1 m
↓ Pb^{208}	stable	

Characteristics of Gamma Radiation

In order to monitor variations of the three radioelements in the ground by airborne gamma ray spectrometry, it is necessary to understand the behaviour of the gamma radiation field. The first theoretical work on the variation in intensity of the natural gamma radiation field with elevation above the surface of the earth was carried out by Eve (1911). He evaluated the intensity of the gamma radiation, measured in terms of the number (n) of ions produced per second per cubic centimetre of air and showed that

$$n = \frac{2\pi Q n_o}{\mu} \int_0^1 e^{-\lambda h/z} dz \qquad (1)$$

where

Q is the mean radium content of the rocks

n_o is the number of ions produced per cubic centimetre per second in air at normal temperature and pressure, one centimetre from one curie of radium,

λ is the linear attenuation coefficient of gamma rays in air,

μ is the linear attenuation coefficient of gamma rays in the ground, and

z is $\sin\theta$, $(\pi/2-\theta)$ being the angle subtended at a detector a distance h above the surface by an elementary ring below the surface.

Gockel (1910) carried out the first airborne experiments to measure the ionizing effect of the gamma radiation from the ground using an electroscope mounted in a balloon and found an erratic variation with altitude, probably because of fluctuations in the concentration of radon daughters in the atmosphere.

Hess (1911, 1912) was the first to obtain definite results using a balloon and showed that while the ionization decreased slightly up to a distance of 1000 m, above 2000 m it began to increase and at 5000 m was two to three times the value found at ground level. These results can be explained if the radon daughter concentration decreases initially with altitude and at the higher elevation the ionization is predominated by cosmic radiation.

Substituting $x = 1/z$ in Equation (1) we arrive at the commonly used expression

$$N = N_o \int_1^\infty \frac{e^{-\lambda h x}}{x^2} dx = N_o E_2(\lambda h) \qquad (2)$$

where

N_o is the count rate with a gamma ray detector at ground level, and

N is the count rate at an altitude h.

The E_2 function is known as the exponential integral of the second kind and in Russian literature is often referred to as the King function. King (1912) generalized Equation (2) and derived the variation of gamma ray intensity, N, with altitude above a circular disc of thickness d subtending an angle 2ϕ at the point of measurement. N is given by

$$N = \frac{2\pi Q n_o}{\mu} \left[E_2(\lambda h) - E_2(\lambda h + \mu d) - \cos\phi \left\{ E_2\left(\frac{\lambda h}{\cos\phi}\right) - E_2\left(\frac{\lambda h + \mu d}{\cos\phi}\right) \right\} \right] \qquad (3)$$

where Q, n_o, μ, h, and λ are the same parameters as in Equation (1).

Table 10B.6

Percentage of detected gamma radiation originated from circular areas beneath the point of detection (altitude 120 m)

Percentage of Infinite Source	Diameter of Circle (m)		
	Potassium[a] (μ = 0.00680/m)	Uranium[a] (μ = 0.00619/m)	Thorium[a] (μ = 0.00506/m)
10	74.5	76.2	79.6
20	110.9	113.3	100.0
30	143.4	146.8	154.1
40	176.1	180.6	190.1
50	211.5	217.2	229.5
60	252.2	259.5	275.5
70	302.7	312.3	333.5
80	372.7	385.8	415.2
90	493.3	513.4	559.5

a – Linear attenuation coefficient taken from Table 1 for air at 0°C and 76 cm Hg.

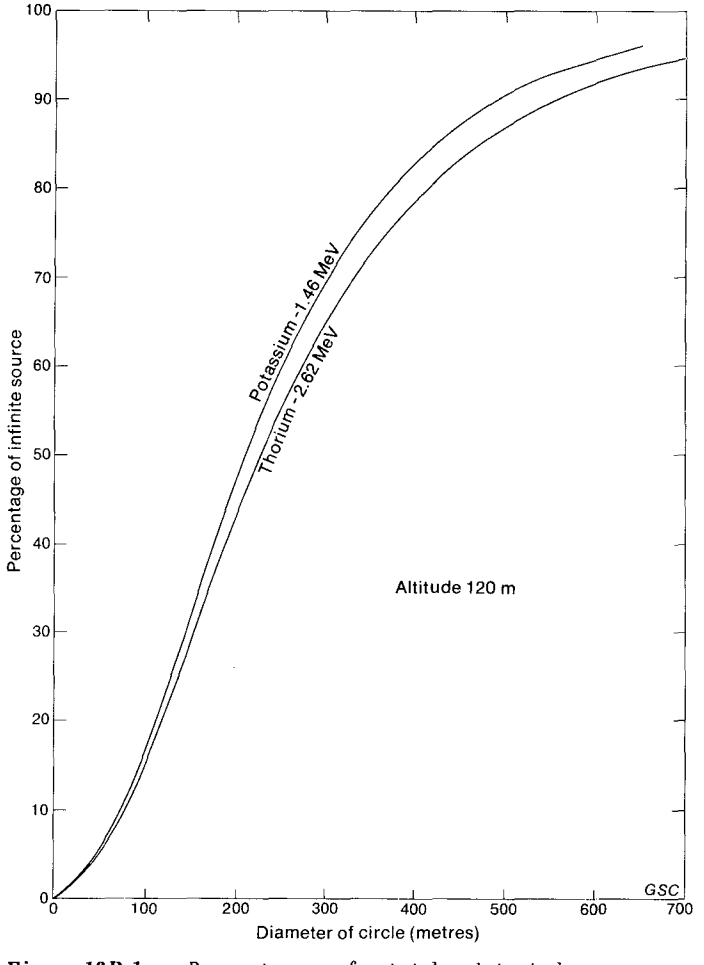

Figure 10B.1. *Percentage of total detected gamma radiation from circular areas beneath the detector.*

It should be pointed out that this expression has been recalculated on many occasions e.g. Godby et al. (1952), Darnley et al. (1968), Duval et al. (1971), Kellogg (1971), and in some instances mathematical or typographical errors have occurred. From this equation it can readily be calculated that the percentage of the total radiation detected, P, originating from a circular area subtended an angle 2ϕ is given by

$$P = 100 \times \frac{\left[E_2(\lambda h) - \cos\phi \; E_2\left(\frac{\lambda h}{\cos\phi}\right)\right]}{E_2(\lambda h)} \quad (4)$$

These results are tabulated in Table 10B.6 for potassium, uranium and thorium gamma ray energies of 1.46, 1.76 and 2.62 MeV and are also illustrated in Figure 10 B.1, for potassium and thorium. However, they are only valid for unscattered mono-energetic gamma radiation, since gamma rayscan be Compton scattered and still contribute to the ionization or be detected by a gamma ray detector.

The complete solution of this gamma ray transport problem is extremely complex since several hundred gamma ray energies are involved, each with different attenuation coefficients and with multiple scattering occurring both in the ground and in the air. However with the advent of high-speed computers the energy and angular distribution of both the direct and scattered gamma ray component can now be evaluated. This has been carried out by Beck and his co-workers at the health and Safety Laboratory in New York (Beck and de Planque, 1968) for the purpose of evaluating the exposure rate from natural gamma radiation and fallout from nuclear weapons tests. Independently Kirkegaard (1972) has carried out similar calculations to aid in the interpretation of gamma ray surveys for exploration and arrived at similar solutions. Both calculation procedures solve the Boltzmann transport equation for two semi-infinite homogeneous media, one being the ground with a uniform distribution of gamma ray emitters and the other being the air. For this particular geometry the mathematics is considerably simplified because of symmetry. They both derive separately the scattered and uncollided gamma ray fluxs.

The continuous nature of the scattered component of the gamma ray flux is illustrated in Figure 10B.2 as calculated by Kirkegaard and Løvborg (1974), for an infinite homogeneous source of 1 per cent potassium, covered with a layer of 20 cm of water which is equivalent to approximately 200 m of air. The scattered component can be seen to increase significantly at energies below about 500 KeV. The calculated results for an infinite source of 1 per cent uranium and 1 per cent thorium are also shown in Figures 10B.3 and 10B.4. Figure 10B.5 shows the energy distribution of the gamma ray flux and its "skyshine" contribution 1 m above a typical granite containing 3.4 per cent potassium, 3 ppm uranium in equilibrium, and 12 ppm thorium (Løvborg et al., 1976). The "skyshine" contribution arises from gamma rays from the ground that have been scattered back towards the ground by the air from heights above 1 m. The "skyshine" flux is predominantly of low energy and contributes approximately 50 per cent of the total flux at energies less than about 200 KeV. At these low energies the radiation is virtually isotropic having a uniform angular distribution, since the gamma rays have suffered multiple collisions and in

Contents

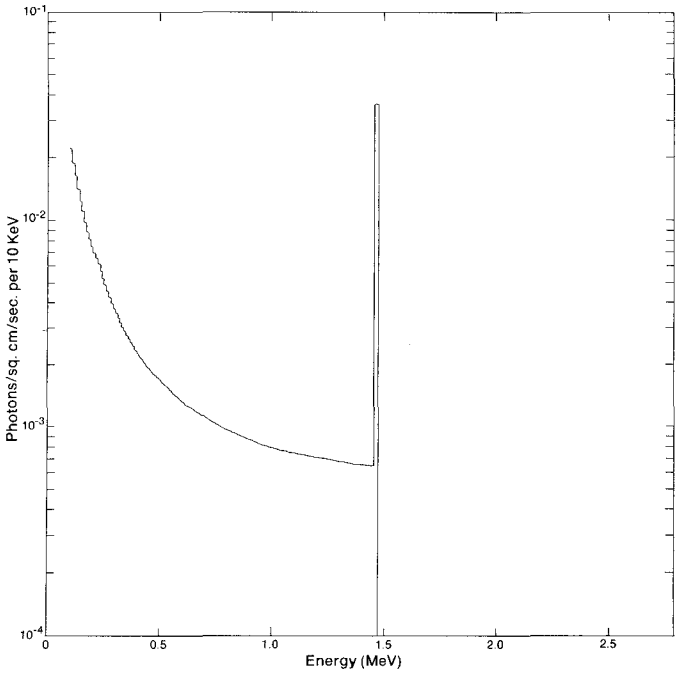

Figure 10B.2. *Energy distribution of the photon flux produced by potassium in sand at a water depth of 20 cm.*

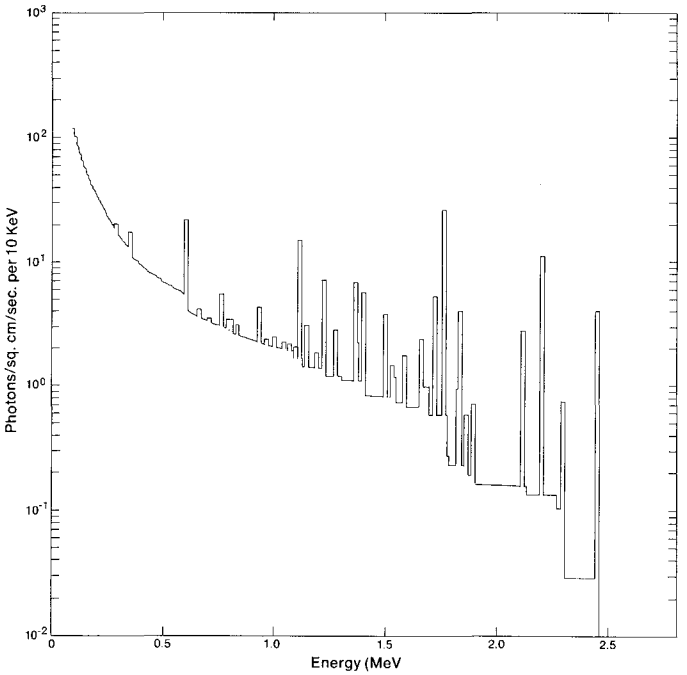

Figure 10B.3. *Energy distribution of the photon flux produced by uranium in sand at a water depth of 20 cm.*

essence lost all knowledge of their original direction. In Figure 10B.6 the angular distribution of a typical gamma ray flux at 1 m illustrates the fact that very little flux comes from sources directly beneath the detector and that the majority of the radiation comes from between 60 and 80° from the vertical (Beck, 1972).

From a knowledge of the energy distribution of the gamma ray flux above the ground containing the different radioelements it is a relatively simple matter to calculate the exposure rate above the ground. Table 10B.7 shows the contribution from potassium, uranium, and thorium to the exposure rate 1 m above the ground. The agreement between the results of Beck et al. (1972) and Løvborg and Kirkegaard (1974) is a good indication that the energy distribution of the gamma ray flux can be derived reliably.

In interpreting airborne gamma ray spectrometry data it is not sufficient to know the gamma ray flux distributions from potassium, uranium, and thorium, since the detector modifies the spectrum considerably. Incorporating the detector response is an extremely complex problem and in general can only be evaluated satisfactorily through a combination of experiment and Monte Carlo simulations. Løvborg and Kirkegaard (1974) have incorporated the detector response of a 7.6 x 7.6 cm (3 x 3 inch) sodium iodide detector and obtained excellent agreement between their theoretical and experimental work.

For a 7.6 x 7.6 cm (3 x 3 inch) detector the energy deposited in the crystal has little dependence on the angle the gamma ray photon strikes the crystal. This is not the case for large diameter crystals commonly used in airborne surveys. In this case it is necessary to derive a detector response which varies with angle. Løvborg et al. (1977) have attempted to do this by making some simplifying assumptions and modifying their theoretical results based on experimental data. From their work they have been able to make estimates of the detector sensitivities and various calibration constants for a variety of cylindrical sodium iodide detectors which are 10.2 cm (4 inches) thick.

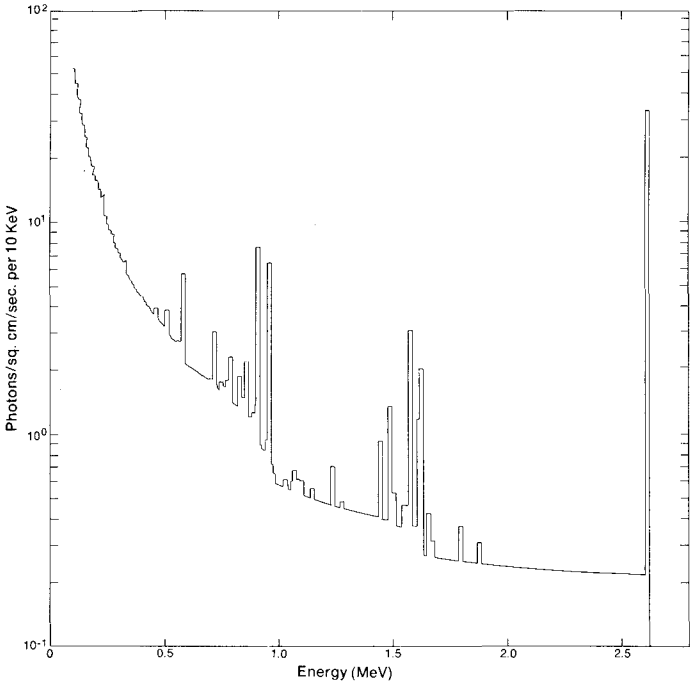

Figure 10B.4. *Energy distribution of the photon flux produced by thorium in sand at a water depth of 20 cm.*

Grasty and Holman (1974) measured the angular sensitivity variation at 2.62 MeV for a variety of detectors commonly employed in airborne survey operation. Grasty (1976a) incorporated these experimental results into the theoretical calculations (Equation (4)) and showed how the percentage contribution of circular areas beneath the aircraft to the total radiation detected varied with detector. These results are presented in Figure 10B.7 for a 29.2 x 10.2 cm (11.5 x 4 inch) and a 12.7 x 12.7 cm (5 x 5 inch) detector. The

Contents

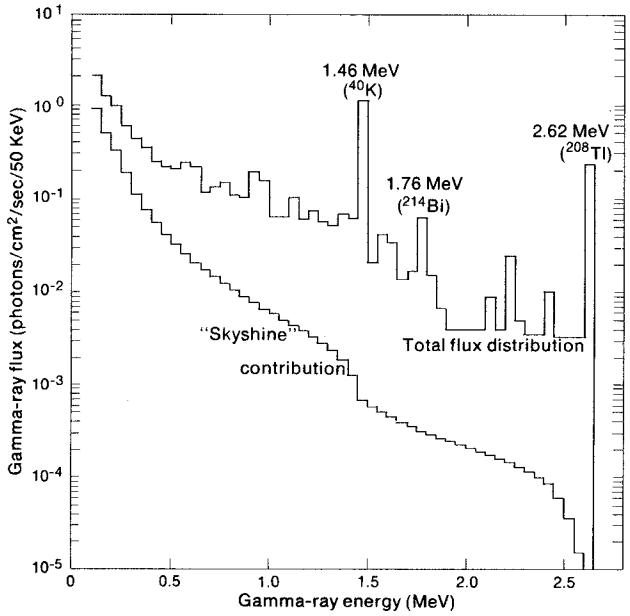

Figure 10B.5. *Energy distribution of the total photon flux and the skyshine component 1 m above a typical granite.*

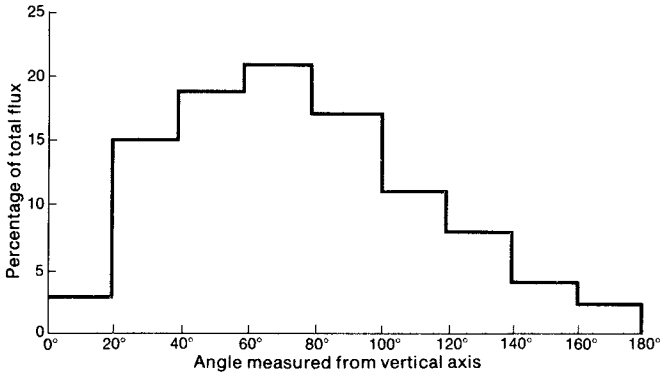

Figure 10B.6. *Angular distribution of the gamma ray flux at 1 m.*

29.2 x 10.2 cm detector has the greatest angular sensitivity variation whereas the 12.7 x 12.7 cm detector shows little angular sensitivity variation. The results show that at these high energies the assumption of a spherical detector is a reasonable approximation even for a 29.2 x 10.2 cm detector. This is because at large angles from the vertical air absorption is significantly more important than the reduced sensitivity of the detector.

OPERATIONAL PROCEDURES

The Airborne System

In aerial measurements of natural radioactivity for geological mapping or uranium exploration, large volume cylindrical sodium iodide detectors are commonly employed. Due to the physical characteristics of the photomultiplier and detector assembly the discrete nature of the unscattered gamma ray photon flux as illustrated in Figures 10B.2 to 10B.4 cannot be observed, and it is necessary to select energy windows which are best representative of the particular radioelements concerned. A typical gamma ray spectrum taken at 120 m is shown in Figure 10B.8 (Foote, 1968). The peaks at 2.62, 1.76, and 1.46 MeV representing

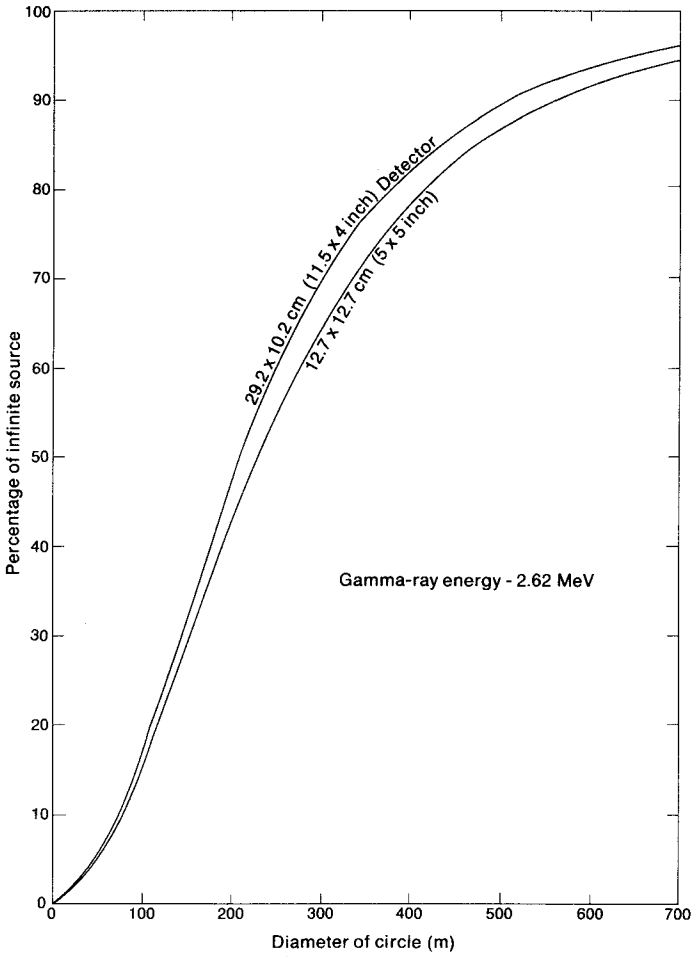

Figure 10B.7. *Percentage of total detected gamma radiation from circular areas beneath two different detectors.*

Table 10B.7

Calculated contributions from potassium, thorium, and uranium to the exposure rate 1 m above soil

	Exposure Rate (μR/h)	
	Løvborg and Kirkegaard (1974)	Beck et al. (1972)
1% K	1.52	1.49
1 ppm Th	0.31	0.31
1 ppm U	0.63	0.62

thallium-208 in the thorium decay series, bismuth-214 in the uranium decay series, and potassium-40, can be readily distinguished. These particular gamma ray photons have been generally accepted as being most suitable for the measurement of uranium and thorium because they are relatively abundant and being high in energy are not appreciably absorbed in the air. They can also be readily discriminated from other gamma rays in the spectrum. Typical gamma ray energy windows for monitoring these particular gamma rays are shown in Table 10B.8. According to McSharry (1973) these particular radioelement windows

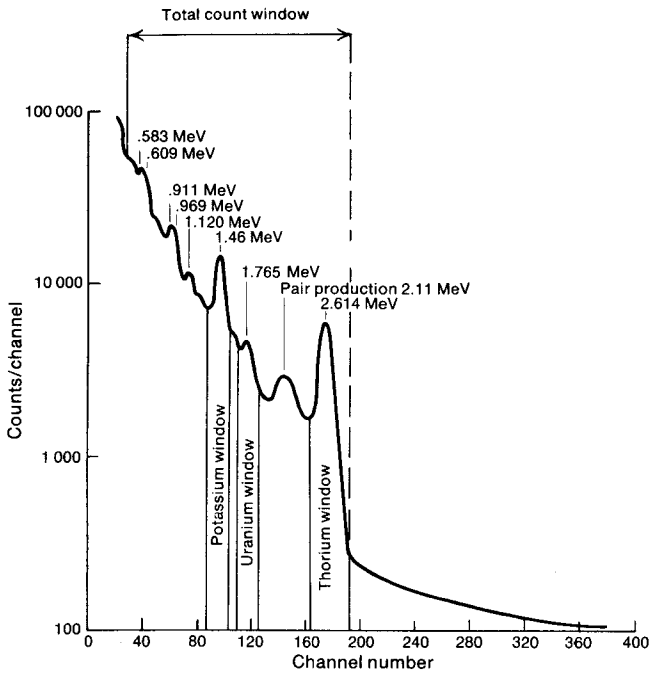

Figure 10B.8. *Typical gamma ray spectrum at 120 m.*

give the most reliable estimates of the individual radioelements. A total count window is also almost always used since the total count reflects general lithological variation and is therefore useful in geological mapping.

In the last few years, full energy spectral recording of up to 512 channels is a common requirement in government contracts for uranium reconnaissance programs and will also certainly become common practice in the future for all airborne surveys. Full spectral recording on magnetic tape has the advantage that subsequent to the survey operations the spectrum can be accurately calibrated from the prominent positions of the potassium and thorium peaks at 1.46 and 2.62 MeV respectively. However until more sophisticated data processing procedures are developed the particular windows shown in Table 10B.8 will be those generally used to convert the airborne data to ground concentrations.

In order to relate the airborne count rates from the three windows to ground concentrations, four particular data processing steps are necessary. These are:

1. the removal of background radiation,
2. a spectral stripping procedure,
3. an altitude correction, and
4. the conversion of the corrected data to ground concentrations.

Background Radiation

In any airborne radioactivity survey three sources of background radiation exist:

1. the radioactivity of the aircraft and its equipment,
2. cosmic radiation, and
3. airborne radioactivity arising from daughter products of radon gas in the uranium decay series.

Table 10B.8

Spectral window widths

Element Analyzed	Isotope Used	Gamma Ray Energy (MeV)	Energy Window (MeV)
Potassium	K-40	1.46	1.37-1.57
Uranium	Bi-214	1.76	1.66-1.86
Thorium	Tl-208	2.62	2.41-2.81
Total Count			0.41-2.81

The radioactivity of the aircraft and its equipment is found to remain constant and is due to the presence of small quantities of natural radioactive nuclides in the detector system and in the airframe. Particularly large contributors can arise from luminous watches and the radium dials on the instrument panels which must be removed from the aircraft.

The cosmic ray background is caused primarily by photons generated by cosmic ray interactions with nuclei present in the air, aircraft or in the detection system itself. The cosmic ray contribution increases with aircraft altitude but shows little variation on a day-to-day basis (Dahl and Odegaard, 1970; Grasty, 1973). Small variations are observed with latitude and with the eleven-year solar cycle and will also vary somewhat with the size of the aircraft. Figure 10B.9 shows a cosmic generated gamma ray spectrum obtained by subtracting over water spectra from two different altitudes (Burson, 1973). The prominent peak near 0.5 MeV is due to the annihilation of positrons created predominantly by pair production from high energy gamma ray photons in the aircraft structure or detector assembly. These positrons annihilate into two gamma ray photons of 0.511 MeV. The cosmic ray contribution in each radioelement window can be removed by monitoring a high-energy window from 3-6 MeV which will be unaffected by natural variations in the ground (Burson, 1973).

By far the most difficult background radiation correction arises from the decay products of radon. Radon, being a gas, can diffuse out of the ground. Furthermore it has a half life of 3.8 days. The rate of diffusion will depend on such factors as air pressure, soil moisture, ground cover, wind, and temperature. The decay products, lead-214 and bismuth-214, are attached to airborne aerosols and consequently their distribution is dependent to a large extent on wind patterns. Under early morning still-air conditions, there can be measurable differences in atmospheric radioactivity at sites a few miles apart. As the day progresses increasing air turbulence tends to mix the air to a greater extent and reduce the atmospheric background close to the ground. Figure 10B.10 shows the morning and afternoon radon concentrations in Cincinnati over a four-year period, taken from the results of Gold et al. (1964). Large annual variations probably arise from the trapping of the radon in the frozen ground during the winter. Darnley and Grasty (1970) reported that on the average 70 per cent of the photons detected in the uranium window arise from radon daughters occurring in the air. Figure 10B.11 shows some typical over water background measurements taken by the Geological Survey of Canada's high sensitivity gamma ray spectrometer while carrying out a large airborne survey in the Northwest Territories of Canada. Typical uranium channel count rates from the ground are around 20 counts/second. It is apparent that the variation of count rate in the total count and potassium window are essentially due to variations of bismuth-214.

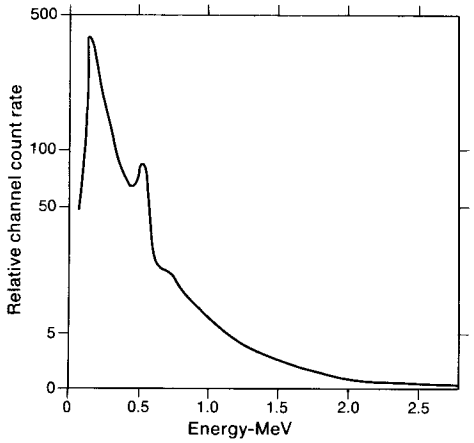

Figure 10B.9. *Cosmic-generated spectrum.*

Problems in measuring the uranium background also arise because of temperature inversions. Figure 10B.12 shows measurements on the same day at different altitudes over Lake Ontario. The thorium channel shows a relatively smooth and expected exponential increase with altitude. The uranium channel shows a general decrease from ground level to 1000 m as has been commonly observed (Hess, 1911, 1912; Burson et al., 1972) but at a temperature inversion at approximately 2000 m the uranium channel increases significantly. Above 2300 m the uranium count rate increases in a similar manner to the thorium channel due to the increasing cosmic ray contribution. From 150 to 300 m the uranium count rate is found to increase since at low altitudes the air cannot be considered as an infinite source (Cook, 1952; Burson et al., 1972).

Since accurate measurements of the count rate in the uranium windows are of prime importance in locating possible uranium targets, it is essential to measure the uranium background as accurately as possible. The technique adopted by the Geological Survey of Canada has been to fly over a lake before the commencement of a survey flight. Since the concentrations of radioactive nuclides in the water are several orders of magnitude lower than that of normal crustal material, the activity measured will be the total background contribution from all three sources. Fortunately in most of Canada lakes are abundant, and the background values can be updated frequently during the course of the survey. Many experimenters have found this method satisfactory when large lakes are present and homogeneous mixing of the radioactive decay products has occurred. An alternative approach when large lakes are not available has been to sample the air by the use of filters (Burson, 1973). Reasonable estimates of the radioactivity of the air can be made from the beta or gamma activity of the dust collected on the filter papers. Foote (1968) used a detector shielded from ground radiation by 10 cm of lead to monitor atmospheric radiation. This procedure has also been employed in Russia, Iran and in the United States (Purvis and Buckmeier, 1969), however the extra detectors and shielding use up valuable space and weight. It is also a complex procedure since gamma rays from the ground can be scattered in the air or in the lead shield and still be detected. Unless the shield is well designed, direct radiation from the ground can also be detected. Unfortunately there is very little documentation on the reliability of this procedure, although in areas with no lakes this may prove to be the only possible technique to use.

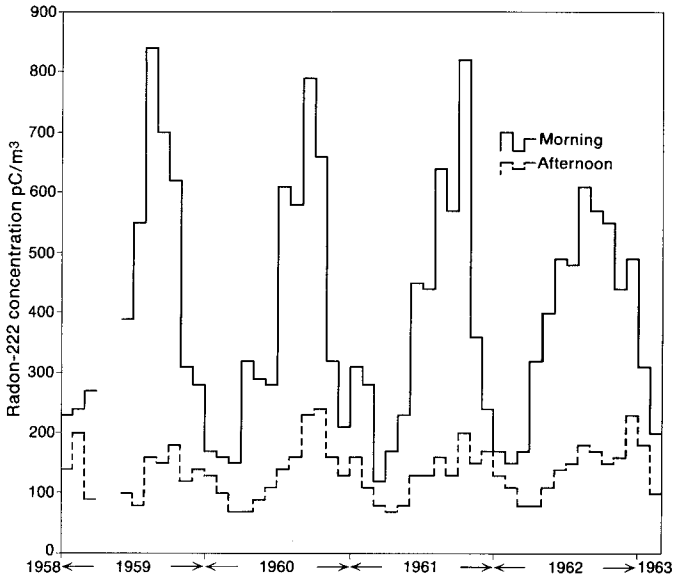

Figure 10B.10. *Monthly average morning (0800 hrs.) and afternoon (1500 hrs.) radon 222 concentrations at Cincinnati.*

Spectral Stripping

Due to Compton scattering in the ground and in the air of 2.62 MeV thallium-208 photons some counts will be recorded in the lower energy potassium and uranium windows from a pure thorium source. Counts in the lower energy windows may also arise from the incomplete absorption of 2.62 MeV photons in the detector or from other lower energy gamma ray photons in the thorium decay series. Similarly counts will be recorded in the lower energy potassium windows from a pure uranium source and can also appear in the high energy thorium window due to high energy gamma ray photons of bismuth-214 in the uranium decay series. Due to the poor resolution of sodium iodide detectors, counts can also be recorded in the uranium channel from a pure potassium source. The ratio of the counts in a lower energy window to those in a high energy window for a pure uranium or thorium source is termed a stripping ratio or spectral stripping coefficient and have generally been called alpha, beta, and gamma where

alpha is the uranium counts per thorium count from a pure thorium source,

beta is the potassium count per thorium count from a pure thorium source, and

gamma is the potassium count per uranium count from a pure uranium source.

Grasty (1977) has adopted the terminology a, b and g for the reverse stripping ratios where

a is the reverse stripping ratio, uranium into thorium,

b is the reverse stripping ratio, potassium into thorium, and

g is the reverse stripping ratio, potassium into uranium.

Unless multiple thorium windows are used, b will have a value of zero.

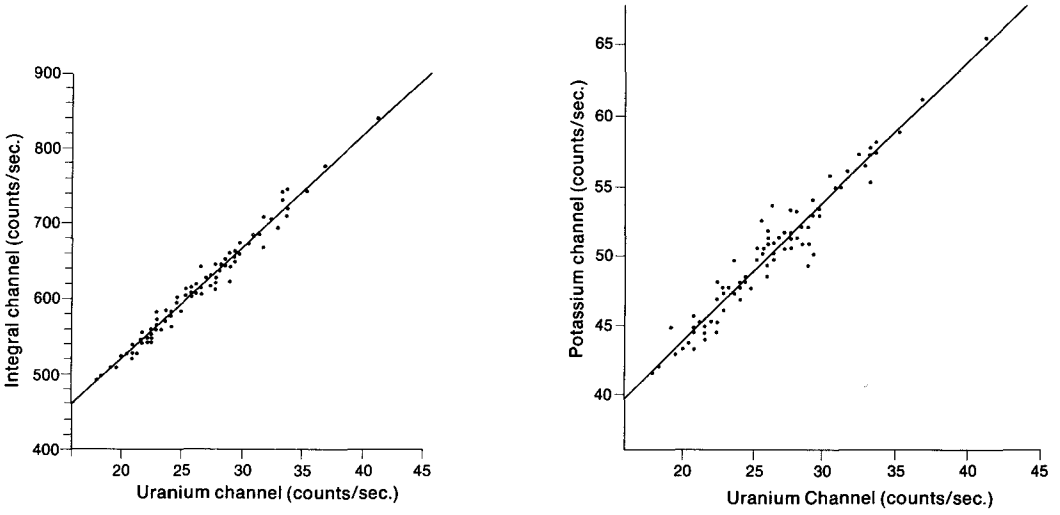

Figure 10B.11. *Variation of over water backgrounds for potassium, uranium and total count.*

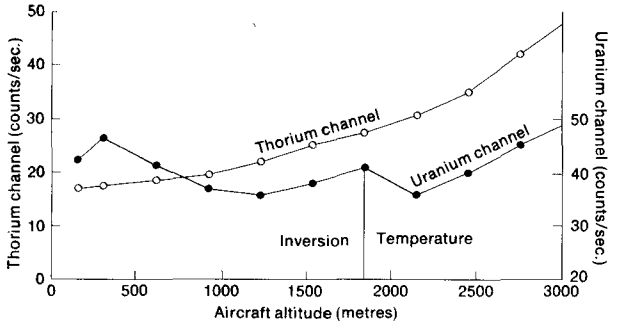

Figure 10B.12. *Variation of uranium and thorium channel count rates over Lake Ontario.*

In order to relate the airborne count rates in the three windows to ground concentrations it is first necessary to determine these six calibration constants. This is generally achieved through the use of large radioactive concrete calibration sources or pads. Sets of these calibration sources have been constructed in Ottawa by the Geological Survey of Canada (Grasty and Darnley, 1971), at Grand Junction for the U.S. Energy Research and Development Agency (Ward, 1978) and also in Iran. The concentration of the Ottawa and Grand Junction pads are given by Killeen (1979).

From measurements on these calibration pads the observed count rates in the three energy windows are all linear combinations of the radioelement compositions of the individual pads. As shown by Løvborg et al. (1972), a general matrix equation can be formulated to relate the observed count rates $N_{2.62}$, $N_{1.76}$ and $N_{1.46}$ to the radioelement concentrations Th_{ppm}, U_{ppm} and K_{pct} of each pad

$$\begin{bmatrix} N_{2.62} \\ N_{1.76} \\ N_{1.46} \end{bmatrix} = \begin{bmatrix} A_{11} & A_{12} & A_{13} \\ A_{21} & A_{22} & A_{23} \\ A_{31} & A_{32} & A_{33} \end{bmatrix} \begin{bmatrix} Th_{ppm} \\ U_{ppm} \\ K_{pct} \end{bmatrix}$$

The matrix coefficients A_{11}, A_{22}, and A_{33} are the sensitivities measured as counts in the thorium, uranium and potassium windows per unit concentration of thorium, uranium and potassium. Expressing this matrix equation as three separate equations (and incorporating background count rates) we obtain for each pad

$$N_{2.62} = A_{11}\,Th_{ppm} + A_{12}\,U_{ppm} + A_{13}\,K_{pct} + B_T \quad (5)$$

$$N_{1.76} = A_{21}\,Th_{ppm} + A_{22}\,U_{ppm} + A_{23}\,K_{pct} + B_U \quad (6)$$

$$N_{1.46} = A_{31}\,Th_{ppm} + A_{32}\,U_{ppm} + A_{33}\,K_{pct} + B_K \quad (7)$$

where B_K, B_U and B_T are the background count rates arising from the radioactivity of the ground surrounding the pads, the radioactivity of the aircraft and equipment, plus the contribution from cosmic radiation and the radioactivity of the air. The calibration constants α, β, and γ, a, b, and g are then related to the various $A_{IJ's}$ by the equations

$$\alpha = A_{21}/A_{11}$$
$$\beta = A_{31}/A_{11}$$
$$\gamma = A_{32}/A_{22}$$
$$a = A_{12}/A_{22}$$
$$b = A_{13}/A_{33}$$
$$g = A_{23}/A_{33}$$

Each of these equations (5, 6 and 7) have four unknowns and consequently from measurements on all five calibration pads the unknowns can be evaluated. Grasty and Darnley (1971) used a standard least squares procedure but have simplified these equations and assumed that there is no interference in the uranium and thorium windows from pure potassium and that any uranium present has little influence on the thorium window i.e. the values of a, b and g are O. In a more recent paper, a is given a value of 0.05 (Grasty, 1975a). Stromswold and Kosanke (1977) used combinations of the pads to arrive at several unique solutions. They then take a weighted average of these results, the weights depending on the estimated accuracy of the individually calculated calibration constants.

It is interesting to note that from the results of background flights over lakes (Fig. 10B.11), the increase in the potassium channel per unit increase in the uranium channel provides a good estimate of the value of the calibration constant γ. Grasty (1975b) has also shown how the value of α can be estimated in areas where the thorium/uranium ratio is high.

The calibration constants derived from the use of these pads are for infinite sources at ground level. Due to Compton scattering in the air the uranium stripping ratio alpha will increase with altitude. Grasty (1975a) derived an analytical solution for the increase of the uranium stripping ratio with altitude. A similar increase with aircraft altitude has been calculated by Løvborg et al. (1977). In the range of altitudes from 50 to 300 m this increase can be approximated by a straight line (Grasty, 1976b).

Altitude Correction

Corrections have to be made to the detector count rates depending on the altitude (h) of the aircraft above the ground. In the range of altitudes normally encountered in airborne survey operations the count rates in each window can be adequately represented by a simple exponential expression in the form

$$N = Ae^{-\mu h} \qquad (8)$$

where A and μ are constants (Darnley et al., 1968; Kogan et al., 1971; Burson, 1973). Figure 10B.13 shows the stripped and background corrected potassium count rate variation with aircraft altitude and the two curves given by Equation (8) and the theoretical expression Equation (2) (Grasty, 1976b).

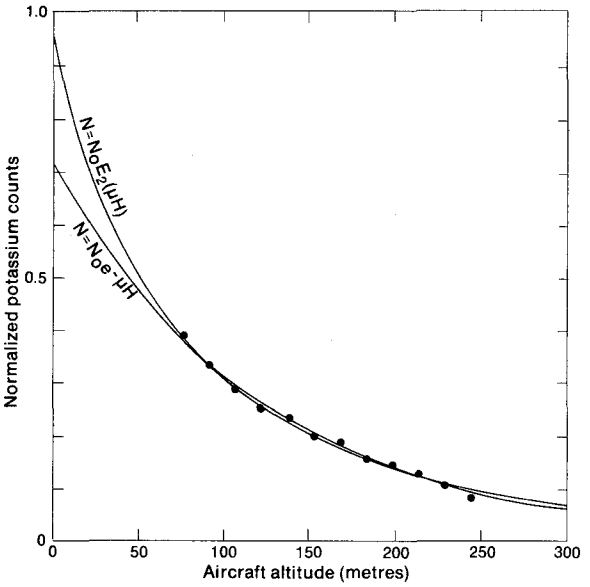

Figure 10B.13. *Potassium variation with aircraft altitude.*

Table 10B.9

Estimated calibration constants for a variety of sodium iodide detectors

Crystal Dimensions (mm)	Stripping Ratio								
	Thorium-into-Uranium (α)			Thorium-into-Potassium (β)			Uranium-into-Potassium (γ)		
	0 m	50 m	125 m	0 m	50 m	125 m	0 m	50 m	125 m
102x102 (4x4 inch)	0.47	0.50	0.53	0.65	0.68	0.73	0.99	1.02	1.07
152x102 (6x4 inch)	0.41	0.44	0.47	0.57	0.59	0.63	0.94	0.97	1.01
229x102 (9x4 inch)	0.39	0.41	0.44	0.52	0.55	0.58	0.90	0.93	0.97
292x102 (11.5x4 inch)	0.37	0.40	0.43	0.50	0.52	0.56	0.88	0.91	0.95

Spectral sensitivities per detector

Crystal Dimensions (mm)	Sensitivity in Counts/Sec Per Radioelement Concentration Unit								
	Potassium Window 1 pct K			Uranium Window 1 ppm eU			Thorium Window 1 ppm eTh		
	0 m	50 m	125 m	0 m	50 m	125 m	0 m	50 m	125 m
102x102 (4x4 inch)	5.7	3.1	1.4	0.52	0.30	0.15	0.26	0.16	0.086
152x102 (6x4 inch)	13	7.1	3.4	1.2	0.70	0.36	0.62	0.39	0.21
229x102 (9x4 inch)	29	16	7.9	2.7	1.6	0.83	1.4	0.90	0.50
292x102 (11.5x4 inch)	47	27	13	4.4	2.6	1.4	2.3	1.5	0.84

Exponential attenuation coefficients for survey heights of 50m and 125m

Crystal Dimensions (mm)	Height Attenuation Coefficients Per Metre x 10^2							
	Potassium Window		Uranium Window		Thorium Window		Total-Count Window	
	50 m	125 m	50 m	125 m	50 m	125 m	50 m	125 m
102x102 (4x4 inch)	1.22	0.97	1.09	0.86	0.96	0.76	0.91	0.73
152x102 (6x4 inch)	1.19	0.95	1.06	0.85	0.94	0.75	0.89	0.72
229x102 (9x4 inch)	1.15	0.94	1.03	0.83	0.90	0.74	0.86	0.71
292x102 (11.5x4 inch)	1.12	0.93	1.01	0.82	0.88	0.73	0.84	0.70

Conversion to Ground Concentration

From flights over a test strip of known ground concentration the sensitivity of the spectrometer in terms of counts per unit concentration per unit time can be readily obtained. The United States Department of Energy has selected a calibration strip near Las Vegas for the purpose of calibrating systems involved in the U.S. National Uranium Reconnaissance program (Geodata International Inc., 1977). The mean concentrations of this strip are 2.4 per cent potassium, 2.8 ppm uranium and 11.6 ppm thorium. This calibration strip suffers from the fact that the ground concentration is not uniform and different concentrations must be assigned to the strip depending on the aircraft altitude and particular detector configuration. The Geological Survey of Canada test strip, a few miles from Ottawa, has concentrations of 2.0 per cent potassium, 0.9 ppm uranium, and 7.7 ppm thorium (Grasty, 1975c; Grasty and Charbonneau, 1974). Because of the low uranium concentration, this strip is not ideal for the accurate calibration of the uranium channel.

Løvborg et al. (1977) have calculated the sensitivities, exponential height correction parameters and stripping ratios, α, β, and γ for four different cylindrical sodium iodide detectors which are 10 cm thick. These results are presented in Table 10B.9 and serve as a useful guide in the design of airborne systems. When the calibration constants for a particular system are known, it is a relatively simple matter to convert the airborne count rates to ground concentrations (Grasty, 1977).

Recommendations for Future Work

Probably one of the most difficult problems to overcome in providing reliable and consistent airborne gamma ray spectrometry data is due to the presence of radon and its decay products in the air. This is particularly true in areas where lakes cannot be found. A systematic study of the use of upward-looking crystals could provide valuable information on the best way of utilizing this particular technique.

In areas with large variations in topographic relief it is common practice to remove the effect of the varying cosmic ray component by monitoring a cosmic ray window from 3-6 MeV. A problem in utilizing this procedure arises because of the low count rate observed in this particular window. A possible procedure which would allow more frequent and accurate updates of the cosmic ray component could be to relate it directly to a barometric altimeter.

Considerable effort is now being spent in uranium reconnaissance programs and it is essential to use systems which are properly calibrated in order that the results from the different systems can be compared. There is considerable difficulty in finding suitable calibration strips which are readily accessible. A possible solution which warrants further attention is to utilize the calibration pads and simulate the absorption effects of the air by covering them with material such as plywood sheet. This technique could well prove to be the most reliable and accurate technique for evaluating the calibration constants for an airborne detection system.

REFERENCES

Beck, H.
1972: The physics of environmental gamma radiation fields; Proceedings of the Second International Symposium on the Natural Radiation Environment, Houston, Texas. J.A.S. Adams, W.M. Lowder, and T.F. Gesell (eds.).

Beck, H., DeCampo, J., and Gogolak, C.
1972: In situ Ge(Li) and NaI(Tl) gamma-ray spectrometry; Rept. HASL-258, U.S. Atomic Energy Comm.

Beck, H. and de Planque, G.
1968: The radiation field in air due to distributed gamma-ray sources in the ground; Rept. HASL-195, U.S. Atomic Energy Comm.

Becquerel, H.
1896a: Sur les radiations invisibles émises par les corps phosphorescents; C.R. Acad. Sci., Paris, v. 122, p. 500-503.

1896b: Sur les radiations invisibles émises par les sels d'uranium; C.R. Acad. Sci., Paris, v. 122, p. 689-694.

Burson, Z.G.
1973: Airborne surveys of terrestrial gamma radiation in environmental research; IEEE Transactions on Nuclear Science, v. NS-21 (1).

Burson, Z.G., Boyns, P.K., and Fritzsche, A.E.
1972: Technical procedures for characterizing the terrestrial gamma radiation environment by aerial surveys; Proceedings of the Second International Symposium on the Natural Radiation Environment, Houston, Texas. J.A.S. Adams, W.M. Lowder, and T.F. Gesell (eds.).

Campbell, N.R.
1907: The β rays from potassium; Proc. Camb. Phil. Soc., v. 14, p. 211.

Campbell, N.R. and Wood, A.
1906: The radioactivity of the alkali metals; Proc. Camb. Phil. Soc., v. 14, p. 15.

Cook, J.C.
1952: An analysis of airborne surveying for surface radioactivity; Geophysics, v. 17 (4), p. 687-706.

Curie, S.
1898: Rayons emis par les composés de l'uranium et du thorium; C.R. Acad. Sci., Paris, v. 126, p. 1101-1103.

Dahl, J.B. and Ødegaard, H.
1970: Areal measurements of water equivalent of snow deposits by means of natural radioactivity in the ground; in Isotope Hydrology, IAEA Vienna, Austria, p. 191-210.

Darnley, A.G., Bristow, Q., and Donhoffer, D.K.
1968: Airborne gamma-ray spectrometer experiments over the Canadian Shield; in Nuclear Techniques and Mineral Resources (International Atomic Agency, Vienna), p. 163-186.

Darnley, A.G. and Grasty, R.L.
1970: Mapping from the air by gamma-ray spectrometry; Proc. Third International Geochemical Symposium, Toronto, Can. Inst. Min. Met. Spec. Vol. 11, p. 485-500.

Duval, J.S., Jr., Cook, B., and Adams, J.A.S.
1971: Circle of investigation of an airborne gamma-ray spectrometer; J. Geophys. Res., v. 76, p. 8466.

Eve, A.S.
1911: On the ionization of the atmosphere due to radioactive matter; Phil. Mag., v. 21, p. 26.

Foote, R.S.
1968: Improvement in airborne gamma radiation data analyses for anomalous radiation by removal of environmental and pedologic radiation changes; in Symposium on the Use of Nuclear Techniques in the Prospecting and Development of Mineral Resources, International Atomic Energy Meeting, Buenos Aires.

Geodata International Inc.
1977: Lake Mead dynamic test range for calibration of airborne gamma radiation measuring systems; ERDA Report GJBX46(77).

Gockel, V.A.
1910: Luftelektrische beobachtungen bei einer Ballonfahrt; Phys. Zeit., v. 11, p. 280-282.

Godby, E.A., Connock, S.H.G., Steljes, J.F., Cowper, G., and Carmichael, H.
1952: Aerial prospecting for radioactive materials; Nat. Res. Coun. Lab. Joint Rept., MR-17 CRR-495, 90 p.

Gold, S., Barkham, H.W., Shlien, B., and Kahn, B.
1964: Measurement of naturally occurring radionuclides in air; The Natural Radiation Environment, Univ. Chicago Press, p. 369-382.

Grasty, R.L.
1973: Snow-water equivalent measurement using natural gamma emission; Nord. Hydr., v. 4, p. 1-16.

1975a: Uranium measurement by airborne gamma-ray spectrometry; Geophysics, v. 40 (3), p. 503-519.

1975b: Uranium stripping determination au naturel for airborne gamma-ray spectrometry; in Report of Activities, Part A, Geol. Surv. Can., Paper 75-1A, p. 87.

1975c: Atmospheric absorption of 2.62 MeV gamma-ray photons emitted from the ground; Geophysics, v. 40 (6), p. 1058-1065.

1976a: The circle of investigation of airborne gamma-ray spectrometers; in Report of Activities, Part B, Geol. Surv. Can., Paper 76-1B, p. 77-79.

1976b: A calibration procedure for an airborne gamma-ray spectrometer; Geol. Surv. Can., Paper 76-16, p. 1-9.

1977: A general calibration procedure for airborne gamma-ray spectrometers; in Report of Activities, Part C, Geol. Surv. Can., Paper 77-1C, p. 61-62.

Grasty, R.L. and Charbonneau, B.W.
1974: Gamma-ray spectrometer calibration facilities; in Report of Activities, Part B, Geol. Surv. Can., Paper 74-1B, p. 69-71.

Grasty, R.L. and Darnley, A.G.
1971: The calibration of gamma-ray spectrometers for ground and airborne use; Geol. Surv. Can., Paper 71-17, 27 p.

Grasty, R.L. and Holman, P.B.
1974: Optimum detector sizes for airborne gamma-ray surveys; in Report of Activities, Part B, Geol. Surv. Can., Paper 74-1B, p. 72-74.

Hess, V.F.
1911: Uber die Absorption der γ-strahlen in der Atmosphare; Phys. Zeit., v. 12, p. 998-1001.

1912: Uber beobachtungen der durchdringenden Strahlung bei sieben Freiballonfahrten; Phys. Zeit., v. 13, p. 1084-1091.

Hubbell, J.H. and Berger, M.J.
1968: Attenuation coefficients, energy absorption coefficients, and related quantities; Engineering Compendium on Radiation Shielding, v. 1, Springer Verlag, Berlin.

Kellogg, W.C.
1971: Calculation of airborne radioactivity survey responses: theory, method, and field test; Annual Meeting of A.I.M.E., New York.

Killeen, P.G.
1979: Gamma ray spectrometric methods in uranium exploration: Application and interpretation; in Geophysics and Geochemistry in the Search for Metallic Ores; Geol. Surv. Can., Econ. Geol. Rept. 31, Paper 10C.

King, L.V.
1912: Absorption problems in radioactivity; Phil. Mag., v. 23, p. 242.

Kirkegaard, P.
1972: Double-P_1 calculation of gamma-ray transport in semi-infinite media; Risø-M-1460.

Kirkegaard, P. and Løvborg, L.
1974: Computer modelling of terrestrial gamma-radiation fields; Risø Report No. 303.

Kogan, R.M., Nazarov, I.M., and Fridman, Sh.D.
1971: Gamma spectrometry of natural environments and formations – theory of the method,applications to geology and geophysics; Israel Program for Scientific Translations, 5778, Jerusalem.

Kolhorster, W.
1928: Gammastrahlen an Kaliumsalzen; Naturwiss, v. 16 (2), p. 28.

Løvborg, L., Grasty, R.L., and Kirkegaard, P.
1977: A guide to the calibration constants for aerial gamma-ray surveys in geoexploration; American Nuclear Society Symposium on Aerial Techniques for Environmental Monitoring, Las Vegas.

Løvborg, L. and Kirkegaard, P.
1974: Response of 3"x3" NaI(Tl) detectors to terrestrial gamma radiation; Nuclear Instruments and Methods 121, p. 239-251, North-Holland Publishing Co.

Løvborg, L., Kirkegaard, P., and Mose Christiansen, E.
1976: The design of NaI(Tl) scintillation detectors for use in gamma-ray surveys of geological sources; IAEA Symposium on Exploration of Uranium Ore Deposits, Vienna.

Løvborg, L., Kirkegaard, P., and Rose-Hansen, J.
1972: Quantitative interpretation of the gamma-ray spectra from geologic formations; Proc. of the Second Int. Symp. on the Natural Radiation Environment, Houston, Texas, J.A.S. Adams, W.M. Lowder, and T.F. Gesell (eds.).

McSharry, P.J.
1973: Reducing errors in airborne gamma ray spectrometry; Austr. Soc. Explor. Geophys. Bull., v. 4 (1), p. 31.

Purvis, A.E. and Buckmeier, F.J.
1969: Comparison of airborne spectral gamma radiation data with field verification measurements; Proc. Sixth Int. Symp. on Remote Sensing of Environment, v. 1.

Rutherford, E.
1903: The magnetic and electric deviation of the easily absorbed rays from radium; Phil. Mag., v. 5, p. 177.

Schmidt, G.C.
1898: Über die von den Thorverbindungen and einigen anderen substanzen ausgehende Strahlung; Ann. d. Phys. u. Chem., v. 65, p. 141.

Smith, A.R. and Wollenberg, H.A.
1972: High-resolution gamma ray spectrometry for laboratory analysis of the uranium and thorium decay series; Proc. 2nd Int. Symp. on the Natural Radiation Environment, Houston, Texas. J.A.S. Adams, W.M. Lowder, and T.F. Gesell (eds.). U.S. Dept. of Commerce, Springfield, Virginia, p. 181-231.

Stromswold, D.C. and Kosanke, K.L.
1977: Calibration and error analysis for spectral radiation detectors; IEEE Nuclear Science Symp., San Francisco, California.

Strutt, R.J.
1903: On the intensely penetrating rays of radium; Proc. Roy. Soc., v. 72, p. 208.

Villard, M.P.
1900: Sur le rayonnement du radium; Comptes Rendus, v. 130, p. 1178.

Ward, D.L.
1978: Construction of calibration facility Walker Field, Grand Junction, Colorado; ERDA Open File GJBX-37(78).

Wulf, V.T.
1910: Beobachtungen uber die Strahlung hoher durchdringungsfahigkeit auf dem Eiffelturm; Phys. Zeit, v. 11, p. 810.

Contents